Annals of Glaciology



Article

Cite this article: van der Laan L, Cholibois K, El Menuawy A, Förster K (2023). A scenario–neutral approach to climate change in glacier mass balance modeling. *Annals of Glaciology* **64**(92), 411–424. https://doi.org/10.1017/aog.2024.22

Received: 31 December 2022
Revised: 24 April 2024
Accepted: 29 April 2024
First published online: 18 October 2024

Keywords:
Climate change; glacier mass balance; glacier modelling

Corresponding author:
Larissa van der Laan;
Email: larissa.vdlaan@nbi.ku.dk

© The Author(s), 2024. Published by Cambridge University Press on behalf of International Glaciological Society. This is an Open Access article, distributed under the terms of the Creative Commons Attribution licence (http://creativecommons.org/licenses/by/4.0/), which permits unrestricted re-use, distribution and reproduction, provided the original article is properly cited.

cambridge.org/aog

A scenario–neutral approach to climate change in glacier mass balance modeling

Larissa van der Laan[1,3], Kim Cholibois[1], Ayscha El Menuawy[1] and Kristian Förster[1,2]

[1]Institute for Hydrology and Water Resources Management, Leibniz Universität Hannover, Hannover, Germany; [2]Institute of Ecology and Landscape, Weihenstephan-Triesdorf University of Applied Sciences, Freising, Germany and [3]Niels Bohr Institute, Copenhagen University, Copenhagen, Denmark

Abstract

Scenario–neutral methods are commonly used to rapidly compare system responses to changes in climate. Using glacier mass balance as a system response, we present a bottom-up, scenario–neutral method as an effective tool for preliminary and overview studies on glacier sensitivity and a complementary approach to traditional top–down methods. The method's main characteristic is its visual result: two–dimensional response surfaces depicting glacier mass balance. Their axes represent perturbations in temperature and precipitation relative to a baseline. The simplicity of our approach makes it applicable to all global glaciers. As a proof–of–concept, the Open Global Glacier Model (OGGM) is used to perform a scenario–neutral glacier sensitivity analysis for four glaciers. In addition, the integration with a top–down approach is demonstrated by overlaying temperature and precipitation from four Coupled Model Intercomparison Project Phase 6 (CMIP6) models, under four Shared Socioeconomic Pathways (SSP). Finally, the benefits of the method are discussed for decision–making and science communication. Assessing results shows that overall, this scenario–neutral method can provide useful information for the research of climate change impact on glacier mass, from aiding study design to science communication.

1. Introduction

Glacier mass change holds global significance as it has far–reaching impacts on sea level, ecosystem hydrology, and the water requirements of communities downstream (Milner and others, 2017; Brighenti and others, 2019; Zemp and others, 2019). Glacier melt was the largest contributor to sea level rise over the 20th century, and is projected to remain a significant contributor throughout the 21st century (Marzeion and others, 2017; Slangen and others, 2017; Farinotti and others, 2019; Frederikse and others, 2020). Moreover, glaciers' water storage capacity makes their monitoring and prediction crucial to water resources management (Jansson and others, 2003; Förster and van der Laan, 2022; Ultee and others, 2022). To predict glacier mass loss for the 21st century, a 'top–down' approach is typically used. Top–down refers to the cascading down of information, resulting in a system response. Glacier models are forced with regional climates, directly or indirectly derived from General Circulation Models (GCM), to simulate glacier mass evolution under imposed scenarios, see e.g. Hock and others (2019) for a comprehensive overview. However, much of the manifestation of specific climate change scenarios is shaped by socioeconomic and political development, introducing uncertainties into scenario projections and impact (Reilly and others, 2001; Kemp and others, 2022). Scenarios start to diverge significantly mid 21st century, after which they dominate the uncertainty in glacier model projections (Hinkel and others, 2019; Marzeion and others, 2020). On the near term, individual models nonetheless produce individual results with the same scenario. This stems from a combination of internal variability and climate model differences and still adds uncertainty to results (Marotzke, 2019).

The uncertainty from top–down approaches can cause difficulties in the interpretation and communication of results for decision–making processes and science communication (Girard and others, 2015). Consequently, there has been a growing effort over the past decade to better integrate top–down and so–called 'bottom–up' approaches, complementing each other's insights (Bhave and others, 2014; Conway and others, 2019). Bottom–up here refers to a focus on sensitivity or vulnerability of a system, accounting for a range of potential climate changes, regardless of specific scenarios and their inherent uncertainties (Guo and others, 2017; Culley and others, 2021). In the field of hydrology and water resources management, especially in addressing extreme events such as floods and droughts, bottom–up approaches, using a number of scenario–neutral methods, have gained traction (e.g. Prudhomme and others, 2010; Guo and others, 2018; Keller and others, 2019; Beylich and others, 2021). A central aspect of these studies involves identifying and focusing on the climate variables to which the system is most sensitive (Girard and others, 2015; Guo and others, 2017). The main benefit of the studies lies in the simple implementation and rapid appraisal of results (Prudhomme and others, 2010). In glaciology, bottom–up approaches often encompass the analysis of glacier sensitivity to climate change: the mass balance change for a given temperature or precipitation change (Anderson and others, 2010). This knowledge is essential to develop and aid the traditional top–down modeling of glacier mass change. Multiple studies of glacier

sensitivity have been conducted over the past few decades, highlighting the impact of geographical location and glacier geometry on sensitivity (Oerlemans and Fortuin, 1992; De Woul and Hock, 2005). These studies generally focus on one or few, often well–documented glaciers, such as Anderson and others (2010) and Kumar and others (2020). They form important initial knowledge for e.g. larger–scale regional studies (top–down) and assessment of climate change hazard risk (direct use of bottom–up results) (De Woul and Hock, 2005; Knight and Harrison, 2023).

The current study presents a bottom–up, scenario–neutral approach with the following aims: (1) to present a simple method for sensitivity analysis of every global glacier, (2) to show the integration with a top–down approach and, (3) to propose method applications to benefit decision–making and communication needs regarding glacier response to climate change. As a proof–of–concept, we focus on four case–study glaciers for which observed mass balance data and previous sensitivity studies exist. We model mass balance using a temperature index model and estimate both overall and seasonal glacier sensitivity, presented visually and numerically. The visual display method is in the form of response surfaces: two–dimensional planes which map a system's response to a variation in the parameters or variables displayed on the axes. In this case, the axes represent the changes in temperature and precipitation relative to a baseline. Visualization through response surfaces is common in scenario–neutral approaches, as seen in for example Culley and others (2016) and Sauquet and others (2019). The numerical representation is through a glacier sensitivity index (GSI). We integrate the scenario–neutral approach with a top–down approach by superimposing temperature and precipitation from four Coupled Model Intercomparison Project Phase 6 (CMIP6) models, driven with four Shared Socioeconomic Pathways (SSP), onto the response surfaces. Finally, we propose the use and interpretation of scenario–neutral results for decision–making practices and climate science communication.

2. Case study sites

To highlight the differences in climate sensitivity between glaciers, we look at four glaciers in different climatic zones: Hintereisferner (Austria), Austre Brøggerbreen (Svalbard, Norway), Abramov Glacier (Kyrgyzstan) and Peyto Glacier (Canada) (Fig. 1). All four glaciers are World Glacier Monitoring Service (WGMS) reference glaciers and have been the subject of numerous glaciological studies throughout the past decades, (e.g. Young, 1981; Dirmhirn and Trojer, 1955; Oerlemans and Fortuin, 1992; Kuhn and others, 1999; Etzelmüller and others, 2000; Denzinger and others, 2021). The availability of data and previous work to understand these glaciers, including their sensitivity, make them ideal proof–of–concept sites for our approach.

2.1 Hintereisferner

Hintereisferner (46.79°N, 10.77°E), located in the Ötztal Alps in Austria, is a clean–ice valley glacier. Its 2011 area was approximately 6.8 km^2, about 15% smaller than in 2001 (Klug and others, 2018). Its elevation ranges from 2430 m a.s.l. at the terminus (in the outline used here, RGI Consortium, 2017) to 3661 m a.s.l. (Wijngaard and others, 2019). The glacier is located in the

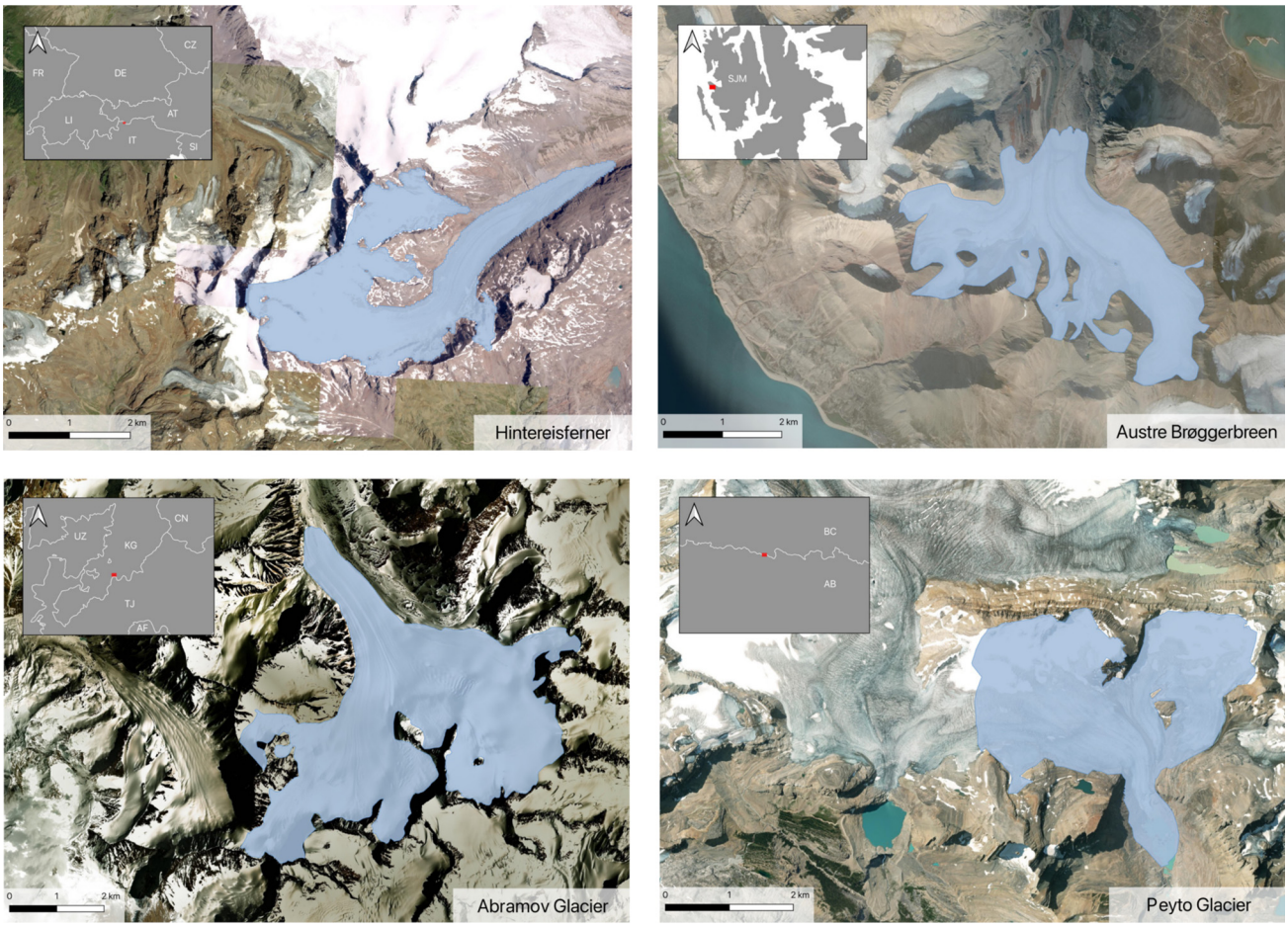


Figure 1. Glacier outlines according to the (RGI Consortium, 2017), from top left in clockwise order: Hintereisferner (Austria), Austre Brøggerbreen (Svalbard, Norway), Abramov Glacier (Kyrgyzstan) and Peyto Glacier (Canada). Inset shows location of the map in their respective country, labels depicting state and/or country codes.

https://doi.org/10.1017/aog.2024.22 Published online by Cambridge University Press

'inner dry Alpine zone', one of the driest places in the European Alps. At the meteorological station in Vent, located 8 km west of the glacier, at 1900 m a.s.l., annual mean precipitation is approximately 750 mm a^{-1} (1987–2016) and annual mean temperature is approximately 3°C (Klug and others, 2018). Most years, annual mean precipitation at the glacier is considerably higher than in Vent, up to double the amount (Fischer, 2013). This is confirmed by precipitation gauge measurements at the glacier and in Vent, see Strasser and others (2018).

2.2 Austre Brøggerbreen

Austre Brøggerbreen (78.89°N, 11.84°E) is a valley/cirque glacier located on the archipelago of Svalbard, Norway. The glacier has an area of 6.1 km^2 (2012), and ranges in elevation from 50 to 650 m a.s.l. (Bruland and Hagen, 2002; RGI Consortium, 2017). Austre Brøggerbreen has lost over 50% of its area since 1936. It is situated in a High Arctic climate, characterized by low temperatures and relatively low precipitation, though the meteorological stations in Longyearbyen and Ny–Ålesund, the latter approximately 4 km from the glacier, show the local climate to be warm compared to other locations between 70 and 80°N (Eckerstorfer and Christiansen, 2011). The mean annual air temperature, measured at the equilibrium line altitude (approximately 300 m a.s.l.), was −8.0°C in the period 1969-1990. In Ny–Ålesund, the mean annual temperature was −5.2°C from 1981–2010, an increase from −6.3°C in the period 1969–1990, due to Arctic amplification (Førland and others, 2011; López-Moreno and others, 2016). Mean annual precipitation in Ny–Ålesund was 385 mm a^{-1} and 427 mm a^{-1} for the periods 1961–1990 and 1981–2010, respectively (Førland and others, 2011).

2.3 Abramov Glacier

The Abramov Glacier (39.60°N, 71.55°E) is a valley glacier in the Koksu Valley, Pamir–Alay range, in Kyrgyzstan. It has an area of 24 km^2 and spans an elevation range of 3650 to 5000 m a.s.l. (in 2015) (Kronenberg and others, 2021). Between 1975 and 2015, the glacier has lost about 5% of its area, and retreated approximately 1 km (Barandun and others, 2015). The Abramov Glacier is located in a continental climate. Mean annual temperature recorded at the glacier meteorological station (3837 m a.s.l.) was −4.1°C for the period 1968–1998 (Kronenberg and others, 2022). Mean annual precipitation was 750 mm a^{-1} from 1968–1998, with maximum precipitation occurring from March to May (Kronenberg and others, 2022).

2.4 Peyto Glacier

Peyto Glacier (51.67°N, –116.54°E) is a mountain glacier located in Banff National Park, Canada. With its continued observation, Peyto Glacier is considered an important 'index glacier for the region' (Kehrl and others, 2014). It had an area of 9.7 km^2 in 2006, and its elevation ranges from 2647 m a.s.l. to 3032 m a.s.l. (Kehrl and others, 2014; Pradhananga and others, 2021). The glacier has continuously been losing mass since at least the 1920s. It is located in a continental climatic regime, characterized by relatively low precipitation inputs and large variability in temperature (Young, 1981). Temperature records from a meteorological station on the glacier, set up and documented by Pradhananga and others (2021), show that the daily average temperature varied between 15°C and −30°C during the period 2013–2018. Records from the closest meteorological station at Bow Summit, approximately 15 km from the glacier, show that total annual precipitation varies between 600 and 1300 mm a^{-1} (Mukherjee and others, 2022).

3. Data and methods

3.1 The open global glacier model

The Open Global Glacier Model (OGGM) is an open–source, modular, numerical model framework with a glacier–centric approach, developed by Maussion and others (2019). It is used to model global past and future glacier evolution. For the current study, we only use OGGM's mass balance model (v. 1.6.0). When using the default pre–processing capabilities, the Randolph Glacier Inventory (RGI) v. 6 provides the glacier outlines used in OGGM, while the digital elevation models are selected per glacier from various available datasets, depending on the region. For the current study, the digital elevation models stem from NASADEM and COPDEM (Crippen and others, 2016; Fahrland and others, 2020, respectively).

As climate input, we use time series of temperature and precipitation from the Climatic Research Unit (CRU) TS v4.01 dataset (Harris and others, 2014). The time series are then downscaled to the CRU 1961–1990 CE climatology (New and others, 2002), which contains elevation data, using the delta method (Ramírez Villegas and Jarvis, 2010; Getahun and others, 2021). This step is necessary because the time series do not contain altitude information, which is needed to compute the temperature at a given glacier elevation.

The temperature and precipitation time series are then applied in a temperature index model, in which monthly mass balance is calculated according to:

$$m_i(z) = p_f P_i^{solid}(z) - \mu^* \max\left((T_i(z) + t_b) - T_{melt}, 0\right). \quad (1)$$

Here, $m_i(z)$ represents the monthly mass balance at altitude z, P_i^{solid} is the solid precipitation, calculated from the total monthly precipitation, according to a temperature threshold, and μ^* is the temperature sensitivity parameter. The temperature threshold used to distinguish between rain and snow assumes that all precipitation is solid when the monthly mean temperature is below 0°C and all precipitation is liquid when the temperature is above 2°C. Between these two temperatures, it is linearly interpolated. p_f is a multiplicative precipitation correction factor and t_b is a temperature bias. The temperature lapse rate is assumed to be −6.5°C km^{-1} and the threshold temperature T_{melt} for melt is assumed to be −1°C.

The current study makes use of the pre–processed OGGM directories, for which the temperature sensitivity parameter, the precipitation factor and the temperature bias are calibrated to match each glacier's observed geodetic mass balance from the dataset by Hugonnet and others (2021). The parameter values from the pre–processed directories are used in the baseline (unperturbed) run of each glacier in this study and can be found in Table 1. For an in–depth description of OGGM, its calibration, characteristics and workflow, please refer to Maussion and others (2019) or https://docs.oggm.org.

3.2 CMIP6 models

For the integration with a top–down approach, we analyze temperature and precipitation from four GCMs, forced with four scenarios, obtained from CMIP6 archived model output. These

Table 1. Parameter values during the unperturbed run and mean glacier sensitivity index GSI_T, for all four glaciers

Glacier	μ^*	p_f	t_b	GSI_T
Hintereisferner	5.0	3.53	1.76	−0.98
Austre Brøggerbreen	5.0	3.35	1.82	−0.41
Abramov Glacier	4.96	4.47	−3.48	−0.53
Peyto Glacier	5.0	3.21	−1.44	−0.56

Units are as follows: temperature sensitivity parameter μ^* (kg m^{-1} day^{-1} K^{-1}), precipitation p_f is a multiplicative factor without a unit, temperature bias t_b (°C) and glacier sensitivity index GSI_T (m w.e. a^{-1}°C^{-1}).

https://doi.org/10.1017/aog.2024.22 Published online by Cambridge University Press

models are FGOALS3, MPI–ESM1, EG–Earth 3 and NorESM2. We use the r1i1p1f1 realization of all models. In order to obtain datasets spanning 2000–2100, we merge GCM output from the CMIP6 experiment 'historical', which spans the years 1850–2015, and GCM output under four SSPs (2015–2100): SSP 1–2.6, 2–4.5, 3–7.0 and 5–8.5 (O'Neill and others, 2016). The SSPs are updated versions of the previous Representative Concentration Pathways (RCP) (van Vuuren and others, 2011). SSPs are driven by emissions and land–use scenarios and refer to climate mitigation, adaptation and impacts. SSP 1–2.6, updated RCP 2.6, refers to a level of radiative forcing of 2.6 Wm^{-2} in 2100 and represents the low end of the future forcing pathways. SSP 2–4.5 (updated RCP 4.5) refers to 4.5 Wm^{-2} as representing the medium level. SSP 3–7.0 is a newly added level at the high end of the range referring to 7 Wm^{-2} radiative forcing in 2100. SSP 5–8.5 (updated RCP 8.5), representing the high end of the future pathways, refers to 8.5 Wm^{-2}.

3.3 Unperturbed baseline climate simulation

In order to create a set of baseline—unperturbed – results, we force the calibrated OGGM mass balance model with the CRU baseline climate described above, 1985–2015. From here on, these runs are referred to as 'unperturbed'. We compute mass balances with fixed glacier geometries, which correspond to the outline at the glacier's RGI dates: Hintereisferner—2003; Austre Brøggerbreen—2007; Abramov Glacier—2000; Peyto Glacier—2004. To ascertain that our baseline results are reliable and the method is transferable to glaciers with little or no observed data, we validate the results against the WGMS observed mass balance data (WGMS, 2022). We assess skill via the calculation and analysis of the mean error, mean absolute error and Pearson correlation. For the mean error, we subtract observed mass balance from modeled mass balance in the same year, for each glacier, over the period 1985–2015 ($N = 107$, because of a lack of observations for the Abramov Glacier from 2000–2012). The mean absolute error is calculated for each glacier based on the absolute differences between the observed and modeled mass balances. The mean absolute error, as it does not take the direction of error into account, provides more information about the magnitude of the discrepancy between modeled and observed values. Finally, we calculate the Pearson correlation coefficient, as a a measure of agreement between simulated and observed mass balance.

3.4 Scenario–neutral approach

Scenario–neutral climate change studies generally describe the effects of climate attribute changes on a system. In such studies, these attributes can change independently, and the impact is not influenced by timing or other variables affecting the system. In our particular case however, because of the impact of temperature on the phase of precipitation, the variables are not fully independent. The disproportionate impact of temperature needs to be taken into account when assessing the magnitude of the impact of precipitation change. However, precipitation also has an isolated effect on mass balance through variations in amount (see Eqn (1)). This is cause for a separate axis in the response surfaces, making the method suitable for mass balance studies.

We analyze the impact of changes in precipitation and temperature, relative to the unperturbed run. We do this in a multitude of combinations, for example a 20% increase in precipitation and no change in temperature, a 10% decrease in precipitation and 5°C increase in temperature, or both attributes remaining at baseline in summer, while changing in winter. These changes are not associated with a particular climate change scenario. The magnitude of the response is a means to assess and convey system sensitivity.

Glacier mass balance is, in reality, also influenced by changes in glacier geometry. This subsequently impacts glacier volume and area. Our simple, fixed geometry approach allows the advantage of modeling glacier response to climate attribute changes under which the real–world glacier would have significantly changed geometry or vanished entirely. For a smaller glacier, the mass balance would be less negative, as a result of changes in geometry. The fixed geometry approach produces mass balance that is termed 'reference surface mass balance' by Elsberg and others (2001), which has a more clear relationship with changes in climate than mass balance computed with changing glacier geometry. For each of the four glaciers in our case study, we employ the following steps towards construction of a scenario–neutral space, outlined in Culley and others (2021):

(1) Selection of Climate Attributes: Temperature and precipitation are the climate attributes selected for our approach. Our choice of climate attributes is forced by the selection of a temperature index model for the calculation of the system response: OGGM's mass balance model, which uses monthly time series of precipitation and temperature as input. This simple method makes it possible to apply the method on a large scale and to regions with a low observational density.
(2) Development of Perturbed Attribute Values: The boundaries and incremental changes of the selected climate attributes are chosen. Since we consider the CMIP6 SSP scenarios until 2100 in the integration of top–down and bottom–up approaches, we use temperature and precipitation from these projections as boundary guidelines. To calculate boundaries for the perturbation of mean annual temperature and annual precipitation, we calculate the difference between the mean values from OGGM baseline climate CRU 1985–2015 and EC–Earth SSP585 values 2070–2100 at the glacier locations. The largest temperature difference is found for Austre Brøggerbreen, with a mean annual temperature over the unperturbed period of −7.2°C and of 3.6°C during 2070–2100. To include this scenario in our boundaries, we apply a perturbation of up to +11°C. For the lower temperature boundary, we include a temperature perturbation of −3°C, to assess the impact of cooling. For total annual precipitation, we use a multiplicative factor rather perturbing by fixed amounts. This takes the large differences in precipitation between the glacier locations into account, making comparison easier. Also here, we find the largest differences from the baseline in SSP585, and in this case for Hintereisferner and Peyto Glaciers. For Hintereisferner, we see a decrease of 10%, from 1480 mm per year to 1310 mm per year between the unperturbed period and 2070–2100. For Peyto Glacier, we see an increase of 48% in precipitation, from 1148 mm per year to 1709 mm per year. To include these scenarios, we apply boundaries of –20% to +50% in precipitation.

    We apply the same method to establish perturbation boundaries for the period 2010–2040, which we look at in the top–down integration. This ensures all CMIP6 scenarios and models are represented within the response surfaces. We note that the boundaries are chosen to incorporate the various SSP scenario ranges, rather than to represent the bounds of plausible changes.
(3) Generation of Perturbed Time Series: To reflect these perturbations in our climate attribute time series, we make use of the temperature bias t_b and the precipitation factor p_f, see Eqn (1). We adjust the temperature bias from the unperturbed run with a specified additive temperature anomaly in °C,

https://doi.org/10.1017/aog.2024.22 Published online by Cambridge University Press

according to the increments on the response surface axes, referred to as the temperature perturbation. Depending on the glacier, we use increments of 0.5°C or 1°C. We adjust precipitation factor p_f with a multiplicative precipitation anomaly, referred to as the precipitation perturbation, in increments of 5% to 10%, depending on the glacier. Also here, the percentages indicated are relative to the unperturbed run. To calculate seasonal sensitivity, during either winter (October–March) or summer (April–September) the climate forcing of one season is that of the unperturbed run, while the climate forcing for the other season is perturbed as described above.

(4) Assessment of System Response: We force OGGM for the period 1985–2015, with the baseline climate and with each incrementally perturbed 30–year time series. This results in an annual mass balance time series over the 30–year time period. From this, we calculate the mean annual mass balance over the time period, which is depicted in the response surface.

3.5 Glacier sensitivity index

To support the visual component of our method, we also calculate a glacier sensitivity index (GSI). This allows comparison with calculated glacier sensitivities from the literature. The GSI builds upon the idea by Oerlemans and Reichert (2000) that mass balance can be related to precipitation and temperature with a sensitivity characteristic. The GSI is calculated per glacier, for perturbations in temperature only. The sole influence of precipitation would be more difficult to quantify in a sensitivity characteristic, as its phase is dependent on temperature.

We only calculate the GSI in instances where temperature is perturbed and precipitation is not, to isolate the temperature perturbation's impact. The calculation is done as follows:

$$GSI_T = (m_k - m_{ref,k})/t_p, \tag{2}$$

in which m_k and $m_{ref,k}$ represent the mass balance in year k of the perturbed run, and year k of the unperturbed run. t_p refers to the temperature perturbation. GSI_T is calculated annually and has the unit of m w.e. $a^{-1}{}^{\circ}C^{-1}$.

The magnitude and the inter–annual variability of the glacier sensitivity index values represent the influence of temperature on mass balance, representing system response. The more negative the GSI, the larger the influence of a temperature perturbation on the system. The larger the variability, the less consistent the influence of temperature changes on the system is.

3.6 Top–down method integration

As a very simple example of combining scenario–neutral methods with a traditional top–down approach, we analyze four CMIP6 models and SSP scenarios, outlined in section CMIP6. For each model and scenario, we calculate the mean annual temperature and annual precipitation over 30 year periods, 2010–2040 and 2070–2100, at the glacier location. The differences between these values and the mean baseline time series are then calculated. These values represent the climate attribute change in the model iteration, relative to the baseline. The results determine the position on the axes and are superimposed onto the response surface. This method is commonly applied in combination with scenario–neutral approaches, see for example Prudhomme and others (2010) and Sauquet and others (2019). The superimposed values serve as an initial assessment of the differences between models and scenarios in the context of the system response, before starting computationally expensive simulations.

4. Results

4.1 Unperturbed run

For the period 1985–2015, we compare modeled mass balances from the unperturbed run to observed mass balances from the WGMS dataset WGMS (2022). We calculate the model performance measures outlined in Table 2. Both individually and averaged over all four glaciers, we see good agreement between modeled and observed mass balances, with the exception of the Abramov Glacier. Averaged over all four glaciers, the mean error is 0.26 ± 0.51 m w.e. a^{-1} and the mean absolute error is 0.48 ± 0.34 m w.e. a^{-1}, affected by the large errors for the Abramov Glacier. For the other three glaciers, the agreement between observed and modeled mass balance is satisfactory (mean error less than 0.2 m w.e. a^{-1}). Overall, the errors are comparable to the error values Eis and others (2021) find for the validation of their mass balance reconstruction of all reference glaciers. Figure 2 shows that the cumulative mass balances, observed and modeled, match well, though the model underestimates the mass balance, for Hintereisferner and Austre Brøggerbreen in particular.

The underestimation of the mass balance for all glaciers can result from the differences between the two datasets of observed mass balance, used in this study. For the development of the pre-processed directories, OGGM is calibrated against geodetic mass balance observations from Hugonnet and others (2021), whereas here, we compare the results from the unperturbed run against the WGMS observed mass balance dataset (WGMS, 2022). Van der Laan and others (2024) compare the two datasets where they overlap, meaning the glacier is included in the geodetic dataset and has annual data in the WGMS dataset. This is the case for 67 glaciers over the period 2000–2019. The mean difference, subtracting mean annual geodetic mass balance from mean annual WGMS mass balance, is –0.11 m w.e. a^{-1}, indicating a systematic difference between the two datasets. This difference is similar in magnitude to the differences between our observed and simulated values for three of the four glaciers, see Table 2. The WGMS mass balances being more negative on the whole can explain the mismatch with a simulation from a model calibrated against the geodetic data. This highlights the potential difficulty in working with pre–calibrated parameters and determining the suitability of a parameter set against an independent dataset.

However, the large errors for the Abramov Glacier cannot be explained through dataset differences alone. For the Abramov Glacier, 13 of the 30 observed years are missing, so it is not possible to show the goodness of fit in terms of cumulative mass balance over the whole period. This is why the years 2011–2015, though observations exist, are removed from Fig. 2. The work by Kronenberg and others (2022) finds that the mass balance of the Abramov Glacier has been predominantly negative since the 1970s. Comparing our results with this study confirms that the positive modeled mass balance in the unperturbed run is incorrect. This is also reflected in the large mean error of 0.63 m w.e. a^{-1}), calculated against the WGMS observed data. The simulated positive mass balance results from the parameter values used for the unperturbed run (Table 1). These parameter values are calibrated for the pre–processed directories to match geodetic mass balance over the reference period 2000–2019 Hugonnet and others (2021). This observed mass balance, of −0.24 m w.e. a^{-1}, is indeed matched when simulating only the period 2000–2019. For our study period of 1985–2015 however, these parameter values cause a systematic cold bias. The calibrated temperature bias, used for the unperturbed run, is −3.5°C. This temperature bias is subtracted from the temperature forcing, which leads to a mean annual forcing temperature of −6.2°C, significantly lower than the observed mean annual temperature at the Abramov Glacier (−4.1°C in 1968–1998 Kronenberg and others,

https://doi.org/10.1017/aog.2024.22 Published online by Cambridge University Press

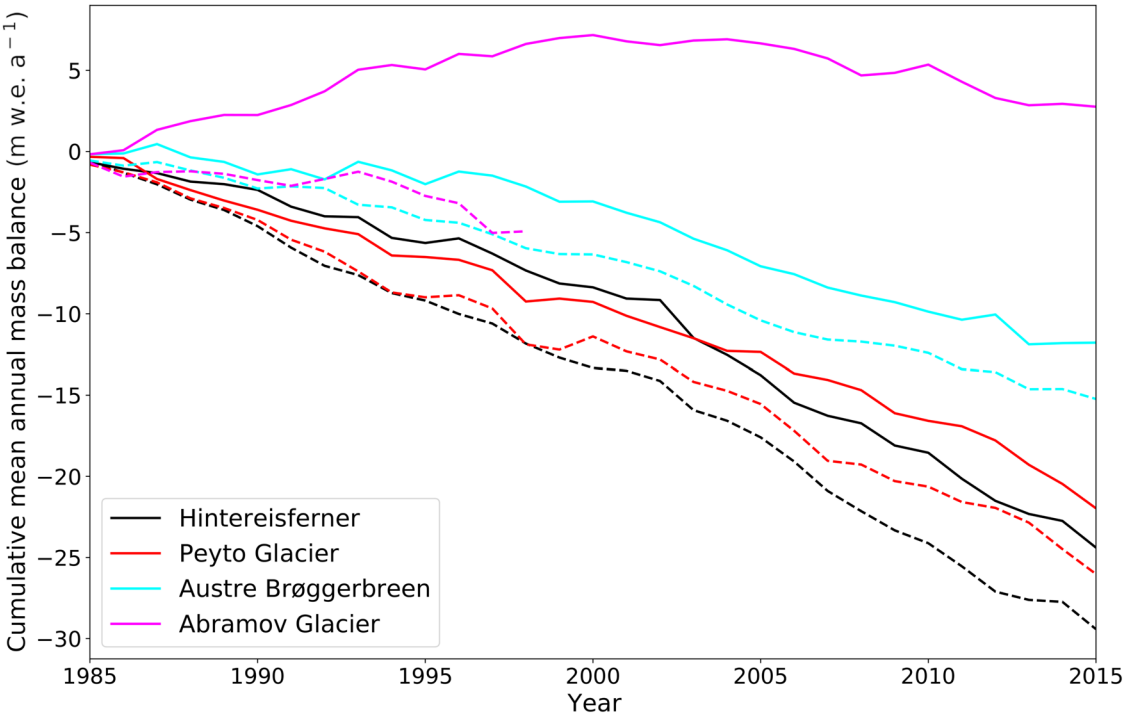


Figure 2. Cumulative mass balance over the period 1985–2015 as simulated with OGGM for the unperturbed run (solid lines), and observed (dashed lines) (WGMS, 2022).

2022). This cold model bias causes an overestimation of the amount of precipitation that falls as snow, and an underestimation of melt. The result is an erroneously positive mass balance. OGGM offers the option to re-calibrate for each glacier, against a variety of datasets, to ensure a better fit for the user's needs. However, doing this for the current study would take away from the main benefit of our method: ease and speed of use for initial studies, for any glacier. Making the choice between re–calibration versus using the out–of–the–box pre–processed directories emphasizes the challenge of balancing complexity and wide applicability.

4.2 Scenario–neutral approach

4.2.1 Overall sensitivity

As outlined above, we generate response surfaces according to the four steps suggested in Culley and others (2021). Using our defined boundaries, this results in a response surface over the period 1985–2015 for Hintereisferner, Austre Brøggerbreen, Abramov Glacier and Peyto Glacier (Fig. 3). We present our results within the context of observed data and results from the literature on their climate and sensitivities.

Hintereisferner responds most sensitively to the changes in climate attributes. In the unperturbed run, mean annual mass balance is −0.97 m w.e. a^{-1}. At the far end of the perturbation boundaries, with a decrease in precipitation of 20% and temperature increase of 11°C, mean annual mass balance goes down to −14.2 m w.e. a^{-1}. Increases in precipitation markedly affect mass balance in the realm of a temperature perturbation of −2°C to 2°C, after which precipitation ceases to have an effect. This is likely due to a removal of accumulation from the mass balance Eqn (1), entirely, as also winter temperatures are above the threshold at which precipitation falls as snow. The fact that the Hintereisferner has the highest amount of annual precipitation confirms the ideas discussed in Meier (1984); Oerlemans and Fortuin (1992) and Oerlemans and Reichert (2000) that sensitivity goes up with precipitation amount, and that generally, glaciers with a higher mass turnover are more sensitive. Hintereisferner's high sensitivity is also conveyed through having the most negative GSI_T (−0.84 m w.e. a^{-1}°C^{-1}—−1.36 m w.e. a^{-1}°C^{-1}). The numbers for the GSI_T are in line with the observed temperature sensitivity for the glacier calculated by Fischer (2010) after 1979, which ranges between −0.38 m w.e. a^{-1}°C^{-1} and −1.54 m w.e. a^{-1}°C^{-1}.

For Austre Brøggerbreen, Elagina and others (2021) find a temperature sensitivity of −0.49 m w.e.a^{-1}°C^{-1}, which is exactly in the GSI_T range we find for the glacier: between −0.33 m w.e. a^{-1}°C^{-1} and −0.57 m w.e. a^{-1}°C^{-1}. Its sensitivity to precipitation decreases with increasing temperature, becoming solely impacted by temperature at a perturbation of 6°C (see Fig. 4). This points to the detrimental effect the process of Arctic amplification will likely have on the glacier's mass balance in the 21st century. The likelihood and magnitude of Arctic amplification for the region is analyzed by van Pelt and others (2021), who find a temperature increase of 6–7°C and 45% increase in precipitation when comparing 1971–2001 observations of Svalbard climate to global and regional projections for Svalbard in 2071–2101.

Table 2. Statistics comparing observed and modeled mass balances from the OGGM unperturbed run, for all four glaciers

Performance measure	Hintereisferner	Austre Brøggerbreen	Abramov Glacier	Peyto Glacier
Mean error (m w.e. a^{-1})	0.11 ± 0.53	0.13 ± 0.54	0.63 ± 0.57	0.16 ± 0.43
Mean absolute error (m w.e. a^{-1})	0.42 ± 0.37	0.31 ± 0.19	0.72 ± 0.23	0.48 ± 0.36
Pearson correlation [p–value]	0.59 [0.0001]	0.48 [0.029]	0.54 [0.00088]	0.67 [0.0049]

All metrics and standard deviations of the metrics are mean values per glacier, calculated over each set of metrics. For the Pearson correlation, the *p*–values have been added in square brackets. The *p*–values, all below 0.05 indicate that all Pearson correlations are statistically significant.

https://doi.org/10.1017/aog.2024.22 Published online by Cambridge University Press

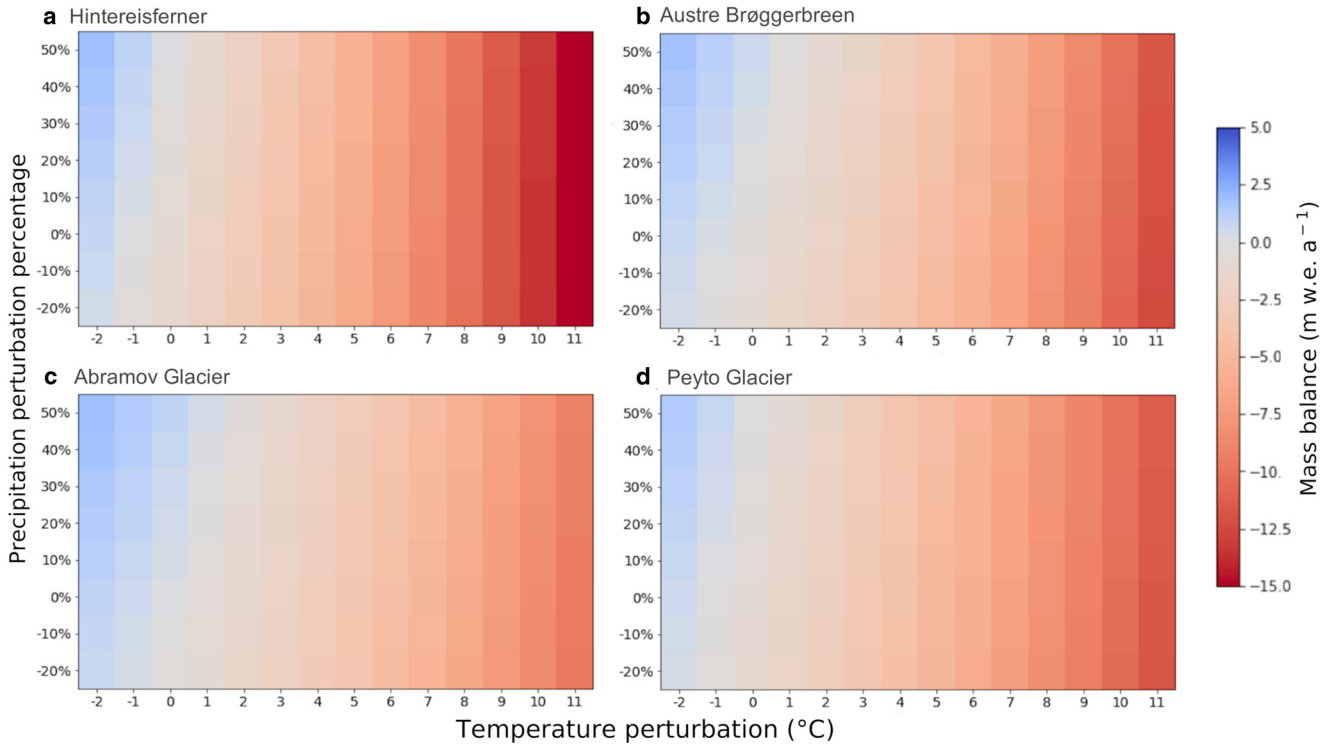


Figure 3. Response surfaces for (a) Hintereisferner, (b) Austre Brøggerbreen, (c) Abramov Glacier and (d) Peyto Glacier, resulting from the fully perturbed time period 1985–2015. Mass balance values represent the annual mean over the 30-year time period. For comparison purposes, the color bars are unified and the transition blue–orange is centered at 0 m w.e. a^{-1}.

Of the four glaciers, the Abramov Glacier has the lowest sensitivity to the changes in climate attributes, with a mean annual mass balance of −6.8 m w.e. a^{-1} at the far end of the perturbations, compared to −14.2 m w.e. a^{-1} for the Hintereisferner. The cold bias in the model, when applied to the Abramov Glacier, causes an erroneously positive mass balance in the unperturbed run. This results in an underestimation of the glacier's sensitivity to temperature perturbations, as it takes much larger perturbations, relative to the unperturbed run, to reach conditions under which mass balance is negative. The cold model bias also causes an overestimation of sensitivity to precipitation, due to a larger fraction of precipitation falling as snow. In spite of this overestimation, like the other three glaciers, Abramov Glacier is sensitive to temperature over precipitation, especially as temperatures increase (Fig. 3). This matches findings by Barandun and others (2015), who note that the Abramov Glacier's sensitivity to summer temperatures is critical to the glacier's mass loss. A study by Wortmann and others (2022) points out that the climate in the glacierized basins of Kyrgyzstan is predicted to become warmer and wetter in the future. But with its low sensitivity to precipitation, this means that even as the climate in Kyrgyzstan gets wetter, it will likely have little positive impact on the glacier's mass balance.

Finally, Peyto Glacier also has a higher sensitivity to temperature than precipitation—with the caveat that the temperature signal is amplified in our method. The GSI_T values for Peyto Glacier vary between −0.48 m w.e. $a^{-1}{}^{\circ}C^{-1}$ and −0.76 m w.e. $a^{-1}{}^{\circ}C^{-1}$. Its sensitivity has been studied by Oerlemans and Fortuin (1992), who conclude that (summer) precipitation does have a significant impact on the addition of mass. This relationship can only be seen at lower temperatures in Fig. 3, where precipitation still falls in solid form. Oerlemans and Fortuin (1992) also note that the impact of summer precipitation is due to the large altitudinal range, which also impacts precipitation state through temperature differences with altitude. As the equilibrium line altitude of Peyto Glacier will likely increase by at least 100 m over the 21st century (Matulla and others, 2008), leaving only 14% of its 1995 area as accumulation zone, this positive impact of summer precipitation will decrease.

4.2.2 Seasonal sensitivity

In addition to overall glacier sensitivity, we calculate seasonal sensitivities (Fig. 4). For clarity, we only discuss the two glaciers with the largest differences in seasonal impact: Hintereisferner and Austre Brøggerbreen. The axes are limited to smaller ranges of perturbations, in order to remain within the bounds of plausibility regarding a change between the typical value for a season and a single outlier. The highest temperature perturbation is of 3°C, which is in line with e.g. the exceptionally warm summer of 2022 in the Alps (Cremona and others, 2023). These heat waves caused the mean annual temperature at the Hintereisferner station to rise to −2.3°C at an altitude of 3245 m a.s.l. (Innsbruck University, 2022). The baseline climate mean annual temperature, over 1985–2015 at Hintereisferner is −1.3°C at 2700 m a.s.l.. Adjusted for altitude, using a lapse rate of 6.5°C km^{-1}, that would correspond to a temperature difference of 2.2 °C, fitting within perturbation limits.

The sensitivity of Austre Brøggerbreen and Hintereisferner to seasonal perturbations differ: when the summer season is unperturbed, mass balance is largely dependent on precipitation for Austre Brøggerbreen, while for Hintereisferner, temperature remains influential (Fig. 4). These results are in line with Oerlemans and Reichert (2000), who observe similar results when comparing Nigardsbreen (Norway) and Franz–Josef Glacier (New Zealand), which have similar differences in their precipitation patterns. When winter is unperturbed, precipitation is of little importance for either glacier, and differences in mass balance are mostly due to temperature changes. Oerlemans and Reichert (2000) do note the importance of Hintereisferner summer precipitation for its mass balance, which we do not observe in our response surfaces. This may be related to using temperature as the sole driver of melt, neglecting other mechanisms such as

https://doi.org/10.1017/aog.2024.22 Published online by Cambridge University Press

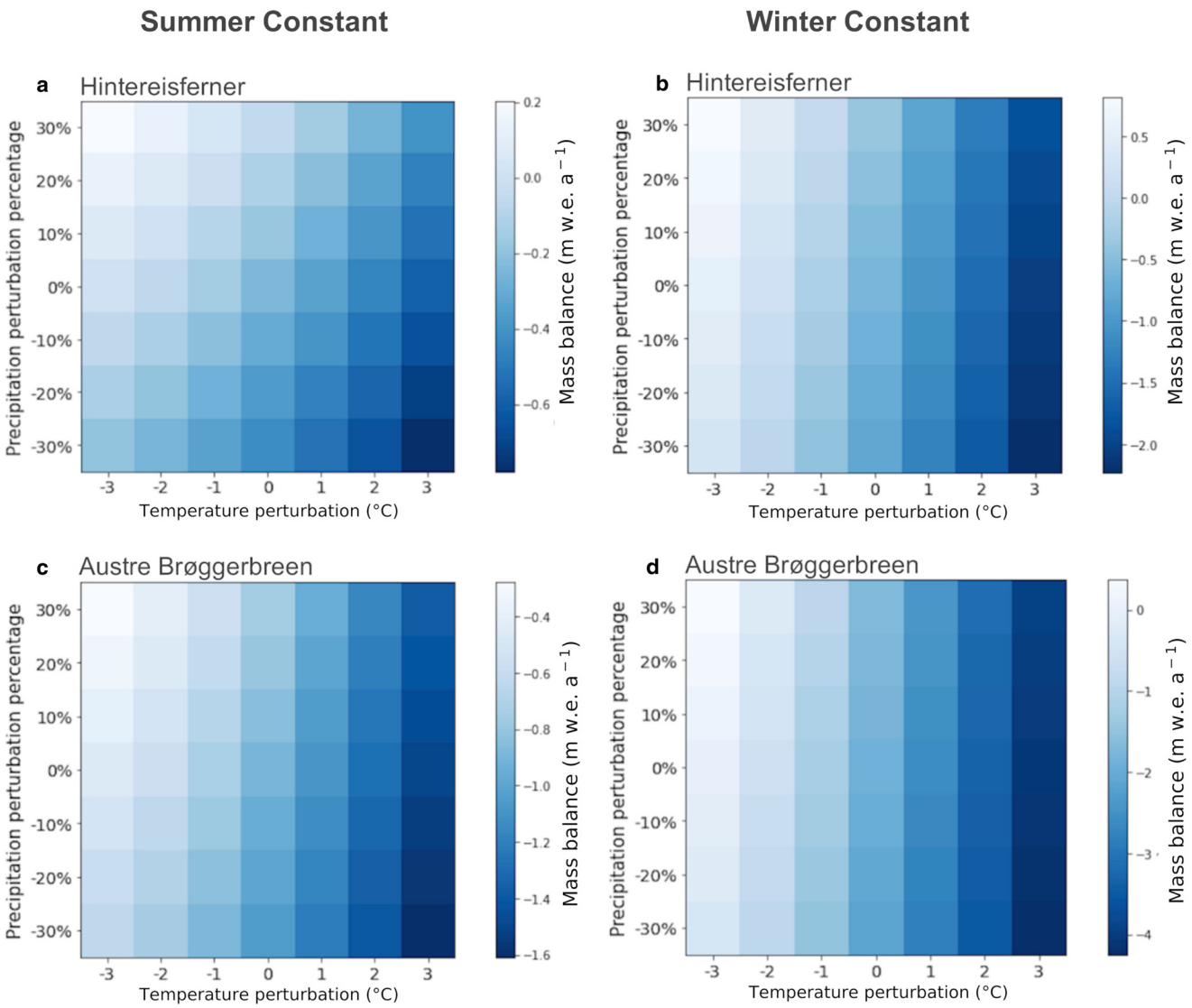


Figure 4. Response surfaces for Hintereisferner (a) and (b) and Austre Brøggerbreen (c) and (d), resulting from the seasonally perturbed time period 1985–2015. The word 'constant' at top of the figure refers to a perturbation of 0 for that season in all years. Mass balance values represent the annual mean over the 30–year time period. The summer contribution to mass balance for 'summer constant' is −0.98 m w.e. a^{-1} for Austre Brøggerbreen (a) and −1.94 m w.e. a^{-1} for Hintereisferner (c). For 'winter constant', the winter contributions to mass balance are 0.43 m w.e. a^{-1} (b) and 0.16 m w.e. a^{-1} (d). For clear contrast of the colors, and thus of the differences per season and glacier, the color scales are not unified, so please note.

albedo change. Another important limitation in the interpretation of these results is the dependence of precipitation state on temperature, amplifying the temperature signal. Overall, the differing seasonal responses of the glaciers are likely due to their location, and how much precipitation falls as snow. For Austre Brøggerbreen, winter precipitation almost solely falls as snow. Perturbations within the boundaries shown here would not affect this (Fig. 4a). For Hintereisferner however, these increases in temperature would affect the fraction of winter precipitation that falls as snow, impacting accumulation and thus mass balance through both temperature and precipitation (Fig. 4c). In summer, temperature changes mainly have an effect on melt, and, of secondary importance, on the state of precipitation. For both glaciers, summer mass balance almost exclusively changes with temperature, affecting the amount of melt. Precipitation has little to no influence, likely because very little summer precipitation falls as snow at these temperatures.

4.3 Top–down method integration

The results of temperature and precipitation differences between climate model iterations and the baseline climate are superimposed onto the response surfaces. This serves as an initial assessment of the climate model iteration, translated into mass balance. Two example results are shown in Fig. 5, for the Hintereisferner and Austre Brøggerbreen glaciers, and the time period 2070–2100. For both glaciers, EC–Earth 3 has the largest increase in temperature and precipitation from the baseline climate, particularly through wet and warm summers. FGOALS 3 projects the lowest increases in temperature, and a decrease in precipitation rather than an increase. NorESM2 and MPI–ESM1 show similar responses, with little change in precipitation. We then translate the GCM differences into system responses. The maximum impact of GCM differences is approximately 4 m w.e. a^{-1} for the Hintereisferner, whereas it is approximately 7 m w.e. a^{-1} for Austre Brøggerbreen. These results can serve as an initial estimate of the uncertainty range, when forcing a glacier model with the GCM time series.

By 2070–2100 however, the present–day geometry used in our OGGM runs would no longer be representative of the glacier state. A response surface for the period 2010–2040, with smaller perturbations on the axes, is depicted in Fig. 6. The differences between the baseline climate and SSP climates are smaller here for temperature, but relatively larger for precipitation. Over this period, the projections have diverged much less than for 2070–2100,

https://doi.org/10.1017/aog.2024.22 Published online by Cambridge University Press

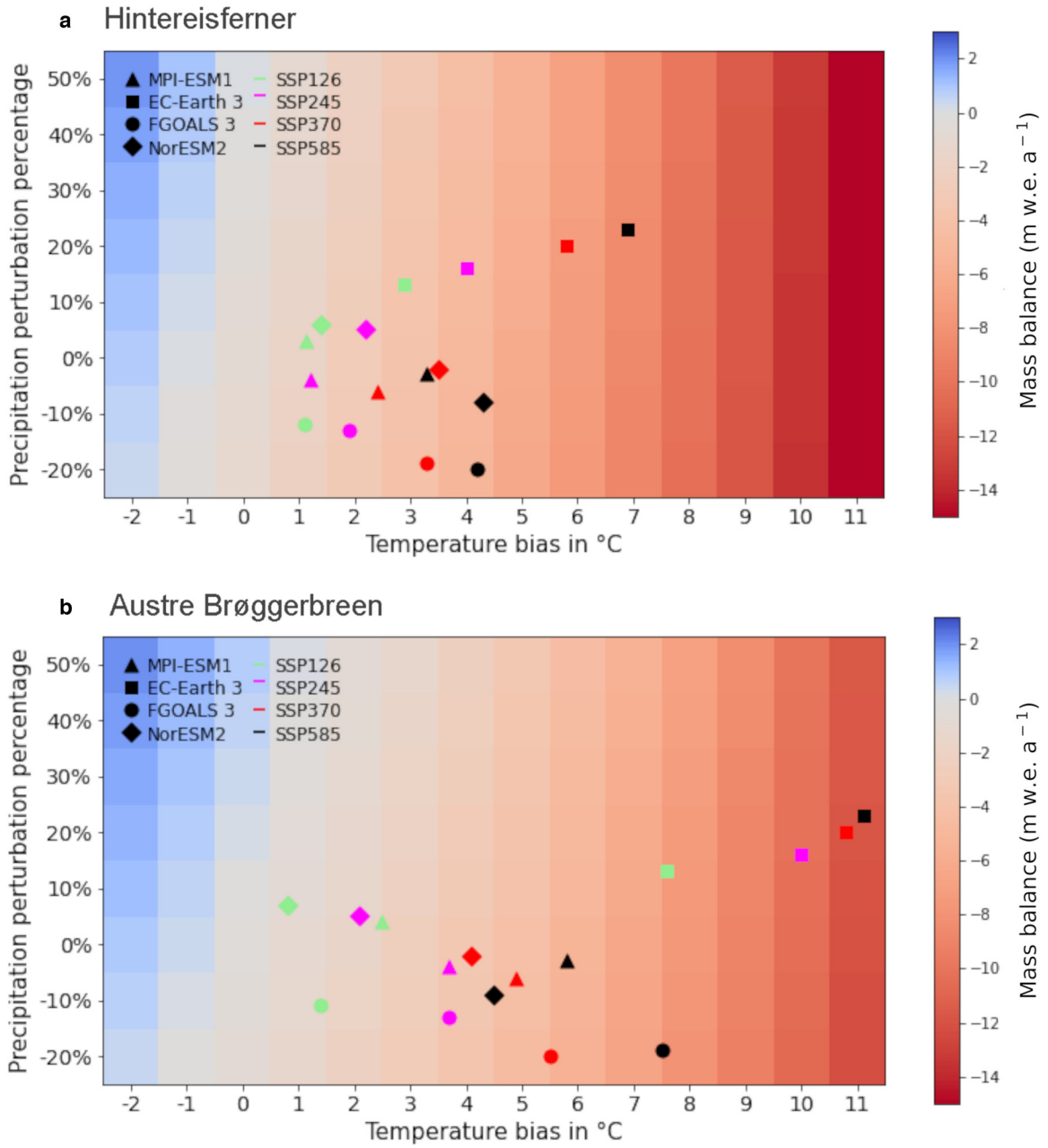


Figure 5. Response surfaces for Austre Brøggerbreen (a) and Hintereisferner (b), with the SSPs for all models overlaid, averaged over the period 2070–2100.

but the differences between models remain consistent. EC–Earth is warmer and wetter than the other models and the scenario divergence is smallest in MPI–ESM1. The maximum impact of model and scenario differences during this time period is about 2 m w.e. a^{-1} for Hintereisferner. For Austre Brøggerbreen, it is much larger, at approximately 8 m w.e. a^{-1}. The study (van Pelt and others, 2021) perform a fixed geometry mass balance simulation, finding a mean Svalbard climatic mass balance of −1.06 m w.e. a^{-1} for 2019–2060 for RCP 8.5. This result is in line with our mass balance ranges for Austre Brøggerbreen for SSP 585 for three of the four models (see Fig. 6). EC–Earth is again an outlier, estimating mass balance to be much more negative. The superimposing of these GCMs shows that, though very simple, the scenario–neutral method can be used to put top–down methods into context.

5. Discussion

The methods applied here depart from the conventionally used top–down approach of modeling glacier response to pre–defined climate change scenarios. We discuss the results in the context of the aims laid out in the introduction.

5.1 Case study application

The first aim is to apply a scenario–neutral approach to four glaciers as a case study, introducing an easy way to study glacier sensitivity, applicable worldwide. The global application is possible because of the availability of pre–processed directories, calibrated glacier–by–glacier. This approach is very simple and does not provide a perfect match between observed/real–world and simulated mass balance for every time period. This is evident from the mean error of 0.63 m w.e. a^{-1} for the Abramov Glacier (2), when simulating the period 1985–2015, whereas the mean error is 0 m w.e. a^{-1} when simulating the reference period 2000–2019. This large possible error and the limitation of static mass balance modeling provide the largest uncertainties in the application of this method. The main benefits of this method are the ease of generation and the global scale. The ability to generate a response surface for

https://doi.org/10.1017/aog.2024.22 Published online by Cambridge University Press

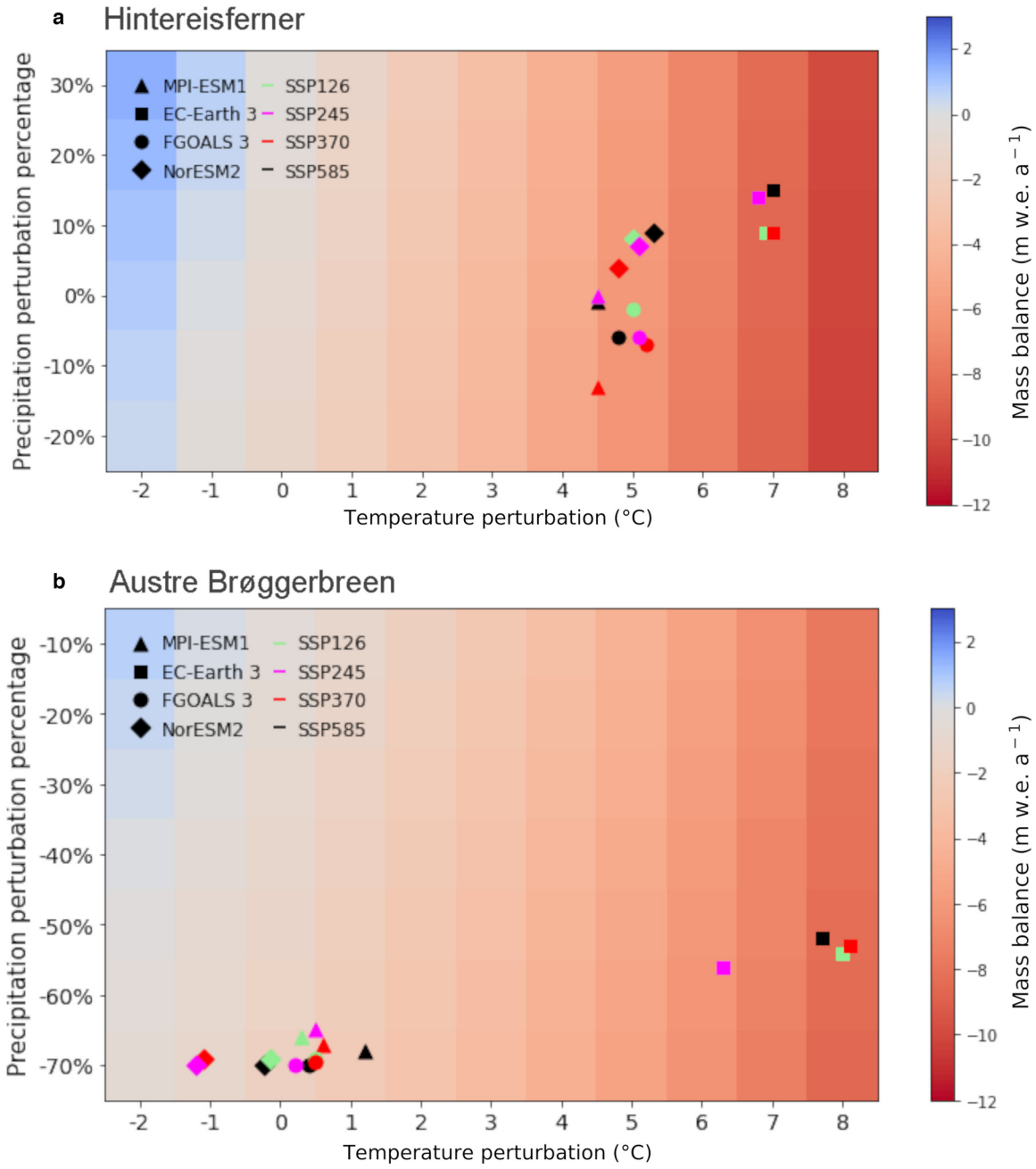


Figure 6. Response surfaces for Austre Brøggerbreen (a) and Hintereisferner (b), with the SSPs for all models overlaid, averaged over the period 2010–2040. Note the difference in precipitation axes for the two glaciers.

every glacier worldwide gives the opportunity to quickly gauge and compare glacier sensitivity for multiple glaciers. Comparing response surfaces at equal climate perturbations makes it possible to rapidly gauge differences between glaciers or at what perturbation X a certain threshold Y would be exceeded. This can also be implemented dynamically, with annual perturbations of temperature and precipitation, modeling glacier area or volume relative to an initial state. Doing this simple analysis for many glacier simultaneously and plotting results together can give a broad, organized overview of glacier response to changes in climate, even in data–sparse regions.

Especially for regions such as New Zealand, where glacier sensitivity has not been widely researched, yet glaciers are highly sensitive (Anderson and others, 2010), this is an advantage for the early stages of study design and can benefit communication with stakeholders. Even though the amount of water stored in New Zealand glaciers only represents 0.15 mm of sea level equivalent, the glaciers are important for hydroelectric power generation in the region (Anderson and others, 2010). The easily interpretable response surfaces clearly convey the impact of climate change to interested decision–makers. Being able to tailor the response surfaces to specific boundaries and local glaciers adds local context, unavailable from many top–down studies (Conway and others, 2019).

5.2 Integration with a top–down approach

The second aim is to show the integration with a top–down approach. This is done in the simple but common manner of superimposing future climate change scenarios onto the response surfaces. The main goal of this particular top–down and bottom–up integration is to gauge the differences between projections and models and have a first translation of perturbations into responses. The differences between the four models and scenarios

https://doi.org/10.1017/aog.2024.22 Published online by Cambridge University Press

point to a high potential uncertainty in the use of climate change projections. The first translation of uncertainties from climate variables to mass balances adds information that a pure local climate comparison would not. The information gained through this integration feeds information back for a top–down approach: it can aid in model and scenario selection for multi–model ensembles or intercomparison studies. On shorter time scales, such as the decadal scale, fixed geometry mass balance still matches observed balances well (van der Laan and others, 2024). In these instances, superimposing scenarios on a response surface can provide a useful first step for dynamical modeling studies, as they can be done before running the computationally expensive impact model. This type of rapid assessment is generally considered the greatest asset of scenario-neutral approaches in climate change studies (Prudhomme and others, 2010; Kay and others, 2014).

Besides feeding back information for top–down approaches, the integration here emphasizes the local characteristics of bottom–up methods. Top–down methods would typically look at a multi–model ensemble mean of results and a larger scale, in terms of system response. In this integration however, the bottom–up characteristics of local response (one glacier) and vulnerability and risk (very negative mass balance at EC-Earth SSPs) are emphasized (Girard and others, 2015). Integrated approaches, even as rudimentary as this one, are an example of how GCMs can inform analysis before being used as model forcing (Brown and Wilby, 2012).

5.3 Benefits to decision–making and communication

The third aim is to outline how this method could benefit decision–making and communication needs regarding glacier response to climate change. For decision–making, its strengths are in the local focus and the method potentially precluding an expensive, top–down climate impact assessment for a decision–maker's risk analysis (Brown and Wilby, 2012). Particularly on the short to medium term, climate assessments are relevant to decision–making (Patro and others, 2018). From our method, especially the seasonal sensitivity component can be useful. By keeping one season unperturbed, the impact of perturbations in the other can be isolated. When keeping perturbation ranges the same, comparisons of responses can be made between glaciers, as is done here for Hintereisferner and Austre Brøggerbreen. This provides insight into the differing importance of single seasons and climate characteristics per glacier. Many mass balance studies, including for some WGMS reference glaciers, only explore annual mass balance and continuous mass balance observations are only available for very few glaciers (Landmann and others, 2021). This limits our ability to determine the sensitivity of glaciers to temperature or precipitation directly. Response surfaces can provide insight into the effects of specific climate variables here, by showing different combinations of perturbed variables along the axes.

A use case example would be water availability for hydropower in the Alps, using seasonal sensitivity analysis. Glacier retreat is the major driver in the reduction of hydropower production in the Italian Alps, making climate change a large risk in decision–making processes in this industry (Patro and others, 2018). The current method can be useful in modeling mass balance for the upcoming season. OGGM would be forced with the known values for the preceding season, an average of previous values for the season to be modeled, and plausible perturbations. This gives a range of outcomes for the upcoming season, independent of scenarios, which is especially important when the preceding season was out of the ordinary. An example is the winter 2022–2023, which was strongly below the 2012–2022 accumulation average for Swiss glaciers (Switzerland, 2022). Seasonal modeling of glaciers with a simple temperature index model, especially for the upcoming season, is difficult because of limited immediate availability of short–term re–analysis or model products of temperature and precipitation. Additionally, it is challenging to predict temperature and precipitation at high elevation and in complex topography (Goger and others, 2016), where glaciers are often located. The current scenario–neutral method can provide an approximation of the upcoming season, resulting in a response surface with the likely boundaries of annual balance after such a dry winter. The results of such a study are especially interesting, but difficult to obtain using top–down methods, on the short–term, to e.g. assess risk of low production for hydropower stakeholders. Overall, for decision–making processes with short lead times, such as hydropower or the planning of artificial snow capacity on glaciers in the ski industry, such rapid and simple forecasts can provide important insights (Doyle, 2014).

As a communication tool, response surfaces provide an intuitive way of understanding glacier responses. In hydrological modeling, they are recognized as a flexible, visual tool to promote understanding (Hirpa and others, 2018). A quantification of glacier sensitivity can be difficult to grasp, especially for a non-specialist. Visual response surfaces for glaciers with different sensitivities make clear how identical perturbations in climate can have non–identical impacts. Climate change is also often perceived as an abstract problem, creating psychological distance between the public and the issue (Weber, 2010; Pahl and others, 2014). A participant or stakeholder is more likely to be moved by climate change impact on a location (glacier) they have visited or live close to (Pahl and others, 2014). This psycho–social effect can heighten urgency and engagement (Luís and others, 2018). The possibility of using this method rapidly, for any glacier in the world, can foster connection with the public through local knowledge. Because of the modular and open–source nature of OGGM, which includes an extensive educational platform (OGGM Edu, OGGM, 2022), the response surface function can be added to the list of model functions and can be included in an easily accessible OGGM (Edu) tutorial. This allows students to generate response surfaces for any glacier they are interested in. Through the response surfaces, glacier sensitivity to climate change can be illustrated, in addition to OGGM Edu applications such as the mass balance simulator. The method can easily be extended from the four glaciers presented here to all glaciers listed in the RGI. This type of visualization of climate science, understandable but backed–up by data and methods, is important for community engagement and learning (Sheppard and others, 2011). The scenario–neutral approach can contribute to this.

5.4 Limitations and outlook

Finally, while scenario-neutral approaches can be useful, there are important limitations to the interpretation of the method presented here. The most limiting factor for both the glacier sensitivity index GSI_T and response surfaces is the difference between fixed geometry mass balance and dynamical mass balance. Especially on longer time scales, mass balances develop with both the climate and the glacier's changes in area, volume and altitude. That is why the response surfaces here cannot be interpreted as the true glacier response to climate change and are mainly useful on shorter time scales.

We also conclude that the GSI_T is a largely unnecessary complication of the method. Excellent work in the quantification of glacier sensitivity has been done by e.g. Oerlemans and Fortuin (1992), Fischer (2010) and more recently Krampe and others (2022). While we have confirmed that calculating the glacier sensitivity index GSI_T works, the utility of the scenario–neutral approach does not lie in the GSI_T but rather in the visual response

https://doi.org/10.1017/aog.2024.22 Published online by Cambridge University Press

surfaces. The choice to not omit the glacier sensitivity index stems solely from its use in comparing results for our case study glaciers to previous literature.

Future applications of scenario–neutral mass balance modeling would mainly benefit from the method's simplicity. This is especially beneficial in three use cases: as an exploratory step when comparing glaciers, sensitivities or fixed scenarios, as an estimation of the upcoming mass balance season and as an educational tool. For the first case, it is beneficial that this approach is simple to implement on a global scale.

6. Conclusion

Overall, scenario–neutral methods can provide a useful, complementary approach to traditional top–down methods. The results for the four case study glaciers suggest the applicability of the method to individual glaciers on a global scale. The main added value of this method lies in its simple application, suitable for use cases like rapid sensitivity comparisons for a multitude of glaciers or the initial design of a study of a data–sparse region. An example of integrating top–down and bottom–up approaches is the overlaying of scenario projections onto response surfaces. This can deliver a first analysis, in which the response surface becomes the framework for comparing models and scenarios. It provides an initial translation of changing climate attributes into responses. For decision–making processes, the method's strengths lie in seasonal approximation, which is difficult to obtain quickly and for the right location using traditional approaches. Especially after a season with uncommon temperatures or precipitation, the scenario–neutral method can provide a first insight into the range of responses for the full year. The ability to apply the approach to a specific, local glacier can have a positive effect on decision–makers' and public engagement. Finally, because of its intuitive visual output, the method presented here can be an important tool for science communication, for example in the Edu section of OGGM. Its simplicity comprises a limitation as well as a benefit. Overall, the scenario–neutral approach in OGGM can provide a complementary and useful approach to glacier mass balance modeling.

Acknowledgements. We would like to thank Lizz Ultee for her advice, motivating words and helpful discussions regarding this project. Thanks also goes out to Fabien Maussion, for building the OGGM community and his constructive comments that helped this research underway. This project was funded by the German Research Foundation, Project GLISSADE, no. 416069075

References

Anderson B and 6 others (2010) Climate sensitivity of a high-precipitation glacier in New Zealand. *Journal of Glaciology* **56**(195), 114–128. doi: 10.3189/002214310791190929

Barandun M and 8 others (2015) Re-analysis of seasonal mass balance at Abramov Glacier 1968–2014. *Journal of Glaciology* **61**(230), 1103–1117. doi: 10.3189/2015jog14j239

Beylich M, Haberlandt U and Reinstorf F (2021) Daily vs. hourly simulation for estimating future flood peaks in mesoscale catchments. *Hydrology Research* **52**(4), 821–833. doi: 10.2166/nh.2021.152

Bhave AG, Mishra A and Raghuwanshi NS (2014) A combined bottom-up and top-down approach for assessment of climate change adaptation options. *Journal of Hydrology* **518**, 150–161. doi: 10.1016/j.jhydrol.2013.08.039

Brighenti S and 5 others (2019) Ecosystem shifts in alpine streams under glacier retreat and rock glacier thaw: a review. *Science of the Total Environment* **675**, 542–559. doi: 10.1016/j.scitotenv.2019.04.221

Brown C and Wilby RL (2012) An alternate approach to assessing climate risks. *Eos, Transactions American Geophysical Union* **93**(41), 401–402. doi: 10.1029/2012eo410001

Bruland O and Hagen JO (2002) Glacial mass balance of Austre Brøggerbreen (Spitsbergen), 1971–1999, modelled with a precipitation-run-off model. *Polar Research* **21**(1), 109–121. doi: 10.3402/polar.v21i1.6477

Conway D and 9 others (2019) The need for bottom-up assessments of climate risks and adaptation in climate-sensitive regions. *Nature Climate Change* **9**(7), 503–511. doi: 10.1038/s41558-019-0502-0

Cremona A, Huss M, Landmann JM, Borner J and Farinotti D (2023) European heat waves 2022: contribution to extreme glacier melt in Switzerland inferred from automated ablation readings. *The Cryosphere* **17**(5), 1895–1912. doi: 10.5194/tc-17-1895-2023

Crippen R and 9 others (2016) NASADEM global elevation model: Methods and progress. doi: 10.5194/isprsarchives-xli-b4-125-2016

Culley S and 7 others (2016) A bottom-up approach to identifying the maximum operational adaptive capacity of water resource systems to a changing climate. *Water Resources Research* **52**(9), 6751–6768.

Culley S, Maier HR, Westra S and Bennett B (2021) Identifying critical climate conditions for use in scenario-neutral climate impact assessments. *Environmental Modelling & Software* **136**, 104948.

De Woul M and Hock R (2005) Static mass-balance sensitivity of Arctic glaciers and ice caps using a degree-day approach. *Annals of Glaciology* **42**, 217–224. doi: 10.3189/172756405781813096

Denzinger F and 7 others (2021) Geodetic mass balance of Abramov Glacier from 1975 to 2015. *Journal of Glaciology* **67**(262), 331–342. doi: 10.1017/jog.2020.108

Dirmhirn I and Trojer E (1955) Albedountersuchungen auf dem Hintereisisferner. *Archiv für Meteorologie, Geophysik und Bioklimatologie, Serie B* **6**(4), 400–416. doi: 10.1007/bf02242745

Doyle C (2014) The impact of weather forecasts of various lead times on snowmaking decisions made for the 2010 Vancouver Olympic Winter Games. *Pure and Applied Geophysics* **171**, 87–94. doi: 10.1007/s00024-012-0609-y

Eckerstorfer M and Christiansen HH (2011) The 'High Arctic maritime snow climate' in central Svalbard. *Arctic, Antarctic, and Alpine Research* **43**(1), 11–21. doi: 10.1657/1938-4246-43.1.11

Eis J, Van der Laan L, Maussion F and Marzeion B (2021) Reconstruction of past glacier changes with an ice-flow glacier model: proof of concept and validation. *Frontiers in Earth Science* **9**, 595755. doi: 10.3389/feart.2021.595755

Elagina N and 6 others (2021) Mass balance of Austre Grønfjordbreen, Svalbard, 2006–2020, estimated by glaciological, geodetic and modeling approaches. *Geosciences* **11**(2), 78. doi: 10.3390/geosciences11020078

Elsberg D, Harrison W, Echelmeyer K and Krimmel R (2001) Quantifying the effects of climate and surface change on glacier mass balance. *Journal of Glaciology* **47**(159), 649–658. doi: 10.3189/172756501781831783

Etzelmüller B and 5 others (2000) Glacier characteristics and sediment transfer system of Longyearbreen and Larsbreen, Western Spitsbergen. *Norsk Geografisk Tidsskrift* **54**(4), 157–168. doi: 10.1080/002919500448530

Fahrland E, Jacob P, Schrader H and Kahabka H (2020) Copernicus dem: Copernicus digital elevation model product handbook. *Report AO/1-9422/18/IL G*. doi: 10.5270/esa-c5d3d65

Farinotti D, Round V, Huss M, Compagno L and Zekollari H (2019) Large hydropower and water-storage potential in future glacier-free basins. *Nature* **575**(7782), 341–344. doi: 10.1038/s41586-019-1740-z

Fischer A (2010) Glaciers and climate change: interpretation of 50 years of direct mass balance of Hintereisferner. *Global and Planetary Change* **71**(1–2), 13–26. doi: 10.1016/j.gloplacha.2009.11.014

Fischer A (2013) Long-term glacier monitoring at the lter test sites Hintereisferner, Kesselwandferner and Jamtalferner and other glaciers in Tyrol: a source of ancillary information for biological succession studies. *Plant ecology & diversity* **6**(3-4), 537–547. doi: 10.1080/17550874.2011.568529

Førland EJ, Benestad R, Hanssen-Bauer I, Haugen JE and Skaugen TE (2011) Temperature and precipitation development at Svalbard 1900–2100. *Advances in Meteorology* **2011**, 1–14. doi: 10.1155/2011/893790

Förster K and van der Laan LN (2022) A review on observed historical changes in hydroclimatic extreme events over Europe. *Climate Impacts on Extreme Weather: Current to Future Changes on a Local to Global Scale*, 131–144. doi: 10.1016/B978-0-323-88456-3.00015-0

Frederikse T and 9 others (2020) The causes of sea-level rise since 1900. *Nature* **584**(7821), 393–397. doi: 10.5194/egusphere-egu2020-7907

Getahun GW, Zewdu EA and Mekuria AD (2021) Statistical downscaling (delta method) of precipitation and temperature for Bilate Watershed,

Ethiopia. *International Journal of Water Resources and Environmental Engineering* **13**(1), 20–29. doi: 10.5897/IJWREE2020.0972

Girard C, Pulido-Velazquez M, Rinaudo JD, Pagé C and Caballero Y (2015) Integrating top–down and bottom–up approaches to design global change adaptation at the river basin scale. *Global Environmental Change* **34**, 132–146. doi: 10.1016/j.gloenvcha.2015.07.002

Goger B, Rotach MW, Gohm A, Stiperski I and Fuhrer O (2016) Current challenges for numerical weather prediction in complex terrain: Topography representation and parameterizations. In *2016 International Conference on High Performance Computing and Simulation (HPCS)*, IEEE. doi: 10.1109/hpcsim.2016.7568428

Guo D, Westra S and Maier HR (2017) Use of a scenario-neutral approach to identify the key hydro-meteorological attributes that impact runoff from a natural catchment. *Journal of hydrology* **554**, 317–330. doi: 10.1016/j.jhydrol.2017.09.021

Guo D, Westra S and Maier HR (2018) An inverse approach to perturb historical rainfall data for scenario-neutral climate impact studies. *Journal of hydrology* **556**, 877–890. doi: 10.1016/j.jhydrol.2016.03.025

Harris I, Jones P, Osborn T and Lister D (2014) Updated high-resolution grids of monthly climatic observations–the CRU TS3.10 dataset. *International Journal of Climatology* **34**(3), 623–642. doi: 10.1002/joc.3711

Hinkel J and 9 others (2019) Meeting user needs for sea level rise information: a decision analysis perspective. *Earth's Future* **7**(3), 320–337. doi: 10.1029/2018ef001071

Hirpa FA, Dyer E, Hope R, Olago DO and Dadson SJ (2018) Finding sustainable water futures in data-sparse regions under climate change: insights from the Turkwel River basin, Kenya. *Journal of Hydrology: Regional Studies* **19**, 124–135. doi: 10.1016/j.ejrh.2018.08.005

Hock R and 7 others (2019) GlacierMIP–a model intercomparison of global-scale glacier mass-balance models and projections. *Journal of Glaciology* **65**(251), 453–467. doi: 10.1017/jog.2019.22

Hugonnet R and 9 others (2021) Accelerated global glacier mass loss in the early twenty-first century. *Nature* **592**(7856), 726–731. doi: 10.1038/s41586-021-03436-z

Innsbruck University A (2022) Temperature data Hintereisis 1. https://www.foto-webcam.eu/webcam/hintereisferner1/, accessed: 2022-12-20.

Jansson P, Hock R and Schneider T (2003) The concept of glacier storage: a review. *Journal of Hydrology* **282**(1-4), 116–129. doi: 10.1016/s0022-1694(03)00258-0

Kay A, Crooks S and Reynard N (2014) Using response surfaces to estimate impacts of climate change on flood peaks: assessment of uncertainty. *Hydrological Processes* **28**(20), 5273–5287. doi: 10.1002/hyp.10000

Kehrl LM, Hawley RL, Osterberg EC, Winski DA and Lee AP (2014) Volume loss from lower Peyto Glacier, Alberta, Canada, between 1966 and 2010. *Journal of Glaciology* **60**(219), 51–56. doi: 10.3189/2014jog13j039

Keller L, Rössler O, Martius O and Weingartner R (2019) Comparison of scenario-neutral approaches for estimation of climate change impacts on flood characteristics. *Hydrological Processes* **33**(4), 535–550. doi: 10.1002/hyp.13341

Kemp L and 9 others (2022) Climate endgame: exploring catastrophic climate change scenarios. *Proceedings of the National Academy of Sciences* **119**(34), e2108146119. doi: 10.1073/pnas.2108146119

Klug C and 8 others (2018) Geodetic reanalysis of annual glaciological mass balances (2001–2011) of Hintereisisferner, Austria. *The Cryosphere* **12**(3), 833–849. doi: 10.5194/tc-12-833-2018

Knight J and Harrison S (2023) The sensitivity and evolutionary trajectory of the mountain cryosphere: implications for mountain geomorphic systems and hazards. *Land Degradation & Development* **34**(9), 2464–2482. doi: doi.org/10.1002/ldr.4630

Krampe D, Arndt A and Schneider C (2022) Energy and glacier mass balance of Fürkeleferner, Italy: past, present, and future. *Frontiers in Earth Science* **10**, 1–25. doi: 10.3389/feart.2022.814027

Kronenberg M, Machguth H, Eichler A, Schwikowski M and Hoelzle M (2021) Comparison of historical and recent accumulation rates on Abramov Glacier, Pamir Alay. *Journal of Glaciology* **67**(262), 253–268. doi: 10.1017/jog.2020.103

Kronenberg M and 5 others (2022) Long-term firn and mass balance modelling for Abramov Glacier in the data-scarce Pamir Alay. *The Cryosphere* **16**(12), 5001–5022. doi: 10.5194/tc-16-5001-2022

Kuhn M and 5 others (1999) Measurements and models of the mass balance of Hintereisisferner. *Geografiska Annaler: Series A, Physical Geography* **81**(4), 659–670. doi: 10.1111/1468-0459.00094

Kumar A, Negi H and Kumar K (2020) Long-term mass balance modelling (1986–2018) and climate sensitivity of Siachen Glacier, East Karakoram. *Environmental Monitoring and Assessment* **192**(6), 368. doi: 10.1007/s10661-020-08323-0

Landmann JM and 5 others (2021) Assimilating near-real-time mass balance stake readings into a model ensemble using a particle filter. *The Cryosphere* **15**(11), 5017–5040. doi: 10.5194/tc-15-5017-2021

López-Moreno J, Boike J, Sanchez-Lorenzo A and Pomeroy J (2016) Impact of climate warming on snow processes in Ny-Ålesund, a polar maritime site at Svalbard. *Global and Planetary Change* **146**, 10–21. doi: 10.1016/j.gloplacha.2016.09.006

Luís S and 9 others (2018) Psychosocial drivers for change: understanding and promoting stakeholder engagement in local adaptation to climate change in three European Mediterranean case studies. *Journal of environmental management* **223**, 165–174. doi: 10.1016/j.jenvman.2018.06.020

Marotzke J (2019) Quantifying the irreducible uncertainty in near-term climate projections. *Wiley Interdisciplinary Reviews: Climate Change* **10**(1), e563. doi: 10.1002/wcc.563

Marzeion B and 5 others (2017) Observation-based estimates of global glacier mass change and its contribution to sea-level change. *Integrative study of the mean sea level and its components* **8**(7), 107–132.

Marzeion B and 9 others (2020) Partitioning the uncertainty of ensemble projections of global glacier mass change. *Earth's Future* **8**(7), e2019EF001470. doi: 10.5194/egusphere-egu2020-5579

Matulla C, Watson E, Wagner S and Schöner W (2008) Downscaled GCM projections of winter and summer mass balance for Peyto Glacier, Alberta, canada (2000–2100) from ensemble simulations with ECHAM5-MPIOM. *International Journal of Climatology* **29**(11), 1550–1559. doi: 10.1002/joc.1796

Maussion F and 13 others (2019) The open global glacier model (OGGM) v1.1. *Geoscientific Model Development* **2019**, 909–931. doi: 10.5194/gmd-12-909-2019

Meier MF (1984) Contribution of small glaciers to global sea level. *Science* **226**(4681), 1418–1421. doi: 10.1126/science.226.4681.1418

Milner AM and 9 others (2017) Glacier shrinkage driving global changes in downstream systems. *Proceedings of the National Academy of Sciences* **114**(37), 9770–9778. doi: 10.1073/pnas.1619807114

Mukherjee K and 5 others (2022) Evaluation of surface mass-balance records using geodetic data and physically-based modelling, Place and Peyto glaciers, Western Canada. *Journal of Glaciology* **69**(276), 1–18. doi: 10.1017/jog.2022.83

New M, Lister D, Hulme M and Makin I (2002) A high-resolution data set of surface climate over global land areas. *Climate Research* **21**(1), 1–25. doi: 10.3354/cr021001

Oerlemans J and Fortuin J (1992) Sensitivity of glaciers and small ice caps to greenhouse warming. *Science* **258**(5079), 115–117. doi: 10.1126/science.258.5079.115

Oerlemans J and Reichert B (2000) Relating glacier mass balance to meteorological data by using a seasonal sensitivity characteristic. *Journal of Glaciology* **46**(152), 1–6. doi: 10.3189/172756500781833269

OGGM (2022) Oggm edu. https://edu.oggm.org/en/latest/, accessed: 2022-12-20.

O'Neill BC and 13 others (2016) The scenario model intercomparison project (ScenarioMIP) for CMIP6. *Geoscientific Model Development* **9**(9), 3461–3482. doi: 10.5194/gmd-9-3461-2016

Pahl S, Sheppard S, Boomsma C and Groves C (2014) Perceptions of time in relation to climate change. *Wiley Interdisciplinary Reviews: Climate Change* **5**(3), 375–388. doi: 10.1002/wcc.340

Patro ER, De Michele C and Avanzi F (2018) Future perspectives of run-of-the-river hydropower and the impact of glaciers' shrinkage: the case of Italian Alps. *Applied Energy* **231**, 699–713. doi: 10.1016/j.apenergy.2018.09.063

Pradhananga D and 8 others (2021) Hydrometeorological, glaciological and geospatial research data from the Peyto glacier research basin in the Canadian Rockies. *Earth System Science Data* **13**(6), 2875–2894. doi: 10.5194/essd-13-2875-2021

Prudhomme C, Wilby RL, Crooks S, Kay AL and Reynard NS (2010) Scenario-neutral approach to climate change impact studies: application to flood risk. *Journal of Hydrology* **390**(3-4), 198–209. doi: 10.1016/j.jhydrol.2010.06.043

Ramírez Villegas J and Jarvis A (2010) Downscaling global circulation model outputs: the delta method decision and policy analysis working paper no. 1. *CIAT Decision and Policy Analysis Working Papers*. https://hdl.handle.net/10568/90731

https://doi.org/10.1017/aog.2024.22 Published online by Cambridge University Press

Reilly J and 5 others (2001) Uncertainty and climate change assessments. doi: 10.1126/science.1062001

RGI Consortium (2017) Randolph Glacier Inventory (RGI) – A Dataset of Global Glacier Outlines: Version 6.0. Technical Report, Global Land Ice Measurements from Space. doi: 10.7265/N5-RGI-60

Sauquet E, Richard B, Devers A and Prudhomme C (2019) Water restrictions under climate change: a Rhône–Mediterranean perspective combining bottom-up and top-down approaches. *Hydrology and Earth System Sciences* **23**(9), 3683–3710. doi: 10.5194/hess-23-3683-2019

Sheppard SR and 7 others (2011) Future visioning of local climate change: a framework for community engagement and planning with scenarios and visualisation. *Futures* **43**(4), 400–412. Special Issue: Community Engagement for Sustainable Urban Futures. doi: 10.1016/j.futures.2011.01.009

Slangen A and 6 others (2017) A review of recent updates of sea-level projections at global and regional scales. *Integrative Study of the Mean Sea level and Its Components* **0**, 395–416. doi: 10.1007/978-3-319-56490-6_17

Strasser U and 9 others (2018) The Rofental: a high Alpine research basin (1890–3770 m asl) in the Ötztal Alps (Austria) with over 150 years of hydrometeorological and glaciological observations. *Earth System Science Data* **10**(1), 151–171. doi: 10.5194/essd-10-151-2018

Switzerland GM (2022) Glamos: Glamos web page. https://www.foto-webcam.eu/webcam/hintereisferner1/, accessed: 2022-12-20.

Ultee L, Coats S and Mackay J (2022) Glacial runoff buffers droughts through the 21st century. *Earth System Dynamics* **13**(2), 935–959. doi: 10.5194/esd-13-935-2022

van der Laan L, Vlug A, Scaife AA, Maussion F and Förster K (2024) Decadal re-forecasts of glacier climatic mass balance. *EGUsphere* **2024**, 1–24. doi: 10.5194/egusphere-2024-387

van Pelt WJJ, Schuler TV, Pohjola VA and Pettersson R (2021) Accelerating future mass loss of svalbard glaciers from a multi-model ensemble. *Journal of Glaciology* **67**(263), 485–499. doi: 10.1017/jog.2021.2

van Vuuren DP and 9 others (2011) RCP2. 6: exploring the possibility to keep global mean temperature increase below 2C. *Climatic Change* **109**(1), 95–116. doi: 10.1007/s10584-011-0152-3

Weber EU (2010) What shapes perceptions of climate change?. *Wiley Interdisciplinary Reviews: Climate Change* **1**(3), 332–342. doi: 10.1002/wcc.41

WGMS (2022) Fluctuations of glaciers database. World Glacier Monitoring Service, Zurich, Switzerland. (doi: 10.5904/wgms-fog-2022-09), accessed: 2023-12-12.

Wijngaard RR and 9 others (2019) Modeling the response of the Langtang Glacier and the Hintereisisferner to a changing climate since the little ice age. *Frontiers in Earth Science* **7**, 143. doi: 10.3389/feart.2019.00143

Wortmann M and 7 others (2022) Projected climate change and its impacts on glaciers and water resources in the headwaters of the Tarim River, NW China/Kyrgyzstan. *Climatic Change* **171**(3), 30. doi: 10.1007/s10584-022-03343-w

Young G (1981) The mass balance of Peyto glacier, Alberta, Canada, 1965 to 1978. *Arctic and Alpine Research* **13**(3), 307–318. doi: 10.2307/1551037

Zemp M and 9 others (2019) Global glacier mass changes and their contributions to sea-level rise from 1961 to 2016. *Nature* **568**(7752), 382–386. doi: 10.1038/s41586-019-1889-5

https://doi.org/10.1017/aog.2024.22 Published online by Cambridge University Press